

Communication

# Fabrication, Evaluation, and Antioxidant Properties of Carrier-Free Curcumin Nanoparticles

Jinwei Wu <sup>1,2,†</sup>, Jiaxin Chen <sup>1,†</sup>, Zizhan Wei <sup>1,2</sup>, Pingchuan Zhu <sup>3</sup>, Bangda Li <sup>1</sup>, Qing Qing <sup>1</sup>, Huimin Chen <sup>1</sup>, Weiyang Lin <sup>4</sup>, Jianyan Lin <sup>2</sup>, Xuehui Hong <sup>5,\*</sup>, Fei Yu <sup>1,2,\*</sup> and Xiao Dong Chen <sup>6</sup>

<sup>1</sup> Medical College, Guangxi University, Nanning 530004, China

<sup>2</sup> The Fourth People's Hospital of Nanning, Nanning 530023, China

<sup>3</sup> State Key Laboratory for Conservation and Utilization of Subtropical Agro-Bioresources, College of Life Science and Technology, Guangxi University, Nanning 530004, China

<sup>4</sup> Guangxi State Key Laboratory of Electrochemical Energy Materials, Guangxi University, Nanning 530004, China

<sup>5</sup> Department of Gastrointestinal Surgery, Zhongshan Hospital of Xiamen University, Xiamen 361005, China

<sup>6</sup> Suzhou Key Lab of Green Chemical Engineering, School of Chemical and Environmental Engineering, College of Chemistry, Chemical Engineering and Materials Science, Soochow University, Suzhou 215123, China

\* Correspondence: hongxu@xmu.edu.cn (X.H.); yufei@gxu.edu.cn (F.Y.)

† These authors contributed equally to this work.

**Abstract:** Curcumin (Cur), a natural hydrophobic polyphenolic compound, exhibits multiple beneficial biological activities. However, low water solubility and relative instability hinder its application in food fields. In this study, carrier-free curcumin nanoparticles (CFC NPs) were prepared by adding the DMSO solution of Cur into DI water under continuous rapid stirring. The morphology of CFC NPs was a spherical shape with a diameter of  $65.25 \pm 2.09$  nm ( $PDI = 0.229 \pm 0.107$ ), and the loading capacity (LC) of CFC NPs was as high as  $96.68 \pm 0.03\%$ . The thermal property and crystallinity of CFC NPs were investigated by XRD. Furthermore, the CFC NPs significantly accelerated the release of Cur in vitro owing to its improved water dispersibility. Importantly, CFC NPs displayed significantly improved DPPH radical scavenging activity. Overall, all these results suggested that CFC NPs would be a promising vehicle to widen the applications of Cur in food fields.

**Keywords:** curcumin; carrier-free; nanoparticles; antioxidant; food



**Citation:** Wu, J.; Chen, J.; Wei, Z.; Zhu, P.; Li, B.; Qing, Q.; Chen, H.; Lin, W.; Lin, J.; Hong, X.; et al. Fabrication, Evaluation, and Antioxidant Properties of Carrier-Free Curcumin Nanoparticles. *Molecules* **2023**, *28*, 1298. <https://doi.org/10.3390/molecules28031298>

Academic Editor: Federica Belluti

Received: 11 December 2022

Revised: 19 January 2023

Accepted: 26 January 2023

Published: 29 January 2023



**Copyright:** © 2023 by the authors. Licensee MDPI, Basel, Switzerland. This article is an open access article distributed under the terms and conditions of the Creative Commons Attribution (CC BY) license (<https://creativecommons.org/licenses/by/4.0/>).

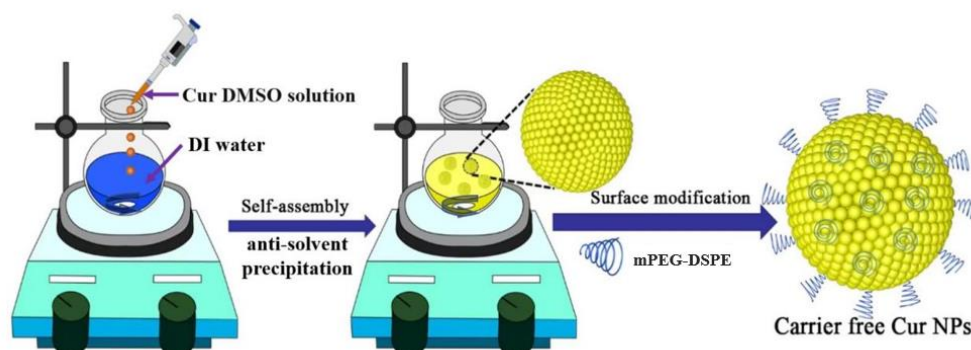
## 1. Introduction

Curcumin (Cur), as a natural pigment, has been widely used as a spice in China and India [1]. Meanwhile, Cur exhibits a wide range of functional and biological features such as antioxidant and antidiabetic properties [2]. Despite its remarkable health benefits, Cur suffers from several limitations in the food and pharmaceutical industries due to its low solubility, poor stability, and rapid metabolism in the body [3]. In response to these problems, many Cur-loaded nanoparticle-based drug delivery systems (DDS) have been exploited in previous works including polymeric nanoparticles, gold nanoparticles, and mesoporous silica nanoparticles [4]. Nevertheless, most of the traditional carrier-assisted drug delivery systems require large quantities of additional excipients, which would induce low drug-loading efficiency [5]. In essence, the drug-loading efficiency of most proposed Cur-loaded nanosized drug delivery systems was less than 10%. Most of these inert carrier materials induce long-term toxicities because of their unclear metabolites [6]. In addition, the use of some carriers results in an undesirable immune response, which impaired the therapeutic effects. High drug-loading nanomedicines should be developed without the use of inert carrier materials [7]; furthermore, the application of many biopolymers (i.e., zein) in the food industry is restricted due to the toxicity of large amounts of organic reagents, as well as the extra cost of removing these organic reagents from the system [8]. It is

important to minimize the use of organic solvents for making commercial food products nowadays [9].

Recently, carrier-free nanodrugs, constructed with amphiphilic drug–drug conjugates or pure drug molecules, have attracted extensive attention because of their easy-making method, excellent drug-loading capability, and the avoidance of large amounts of organic reagents [10]. As an emerging generation of DDS, carrier-free nanodrugs displayed many advantages: (i) excellent drug loading capacity (usually >90%); (ii) no carrier-induced immunogenicity and toxicity; (iii) avoiding any high energy-consuming machine in the preparation of carrier-free nanodrugs [11]; (iv) without using complicated procedures for preparing carriers; and (v) being suitable for most small chemical drug molecules. Zhao et al. reported the carrier-free 7-ethyl-10-hydroxycamptothecin/chlorin e6 nanoparticles by the self-assembly of pure drugs, which exhibited increased inhibition to cancer cells and realized an excellent antitumor effect in vitro [10]. Although this strategy has been widely applied in anti-tumor drugs, few nutraceutical-based carrier-free nanodrugs have been reported.

In this study, CFC NPs were developed via the anti-solvent precipitation method (Scheme 1). During its self-assembly process, a tiny amount of mPEG-DSPE was used for the surface modification of pure CFC NPs [12]. The surface charge, mean particle size, and loading capacity of CFC NPs were systematically investigated. The physico-chemical properties of the CFC NPs were also assessed by XRD, UV-Vis spectrum, TEM, SEM, and fluorescence spectrum. Furthermore, in vitro release profiles of Cur in simulated gastrointestinal fluids and the antioxidant activity of the CFC NPs were carefully evaluated [13].



**Scheme 1.** Schematic illustration of the CFC NPs.

## 2. Results and Discussion

### 2.1. Preparation and Characterization of CFC NPs

The CFC NPs were prepared by the anti-solvent precipitation method, which was displayed in Scheme 1. Firstly, the organic solvent (DMSO) was used to dissolve the Cur. Then, the DMSO solution of Cur was dropped into the DI water (non-solvent for Cur) with vigorous stirring. It should be noted that the supersaturated conditions of the Cur in the water phase would induce the precipitation or nucleation of the CFC NPs. Eventually, the Cur molecules self-assembled into nanoparticles with the driving forces of various noncovalent interactions. Furthermore, the amphiphilic stabilizer (mPEG-DSPE) was added to overcome the agglomeration of CFC NPs due to the supersaturation.

As shown in Figure 1A,B, TEM and SEM indicated that the morphology of CFC NPs was nearly spherical, and the size of the morphological observation was basically consistent with the DLS results. In addition, CFC NPs were well dispersed on the support film, which might be ascribed to enhanced surface hydrophilicity after the addition of mPEG-DSPE. Furthermore, the obvious advantage of carrier-free nanodrug delivery systems is their high drug-loading capacities, usually ranging from 50% to 100% [14]. In this work, the loading capacity of CFC NPs was  $96.68 \pm 0.03\%$ . As shown in Figure 1C, the average size of CFC NPs was  $65.25 \pm 2.09$  nm with a narrow particle size distribution ( $0.229 \pm 0.107$ ),

which proved the uniform property of CFC NPs [15]. Meanwhile, the zeta potential ( $-20.5 \pm 1.3$  mV) of CFC NPs was high enough to prevent aggregation of CFC NPs [16].

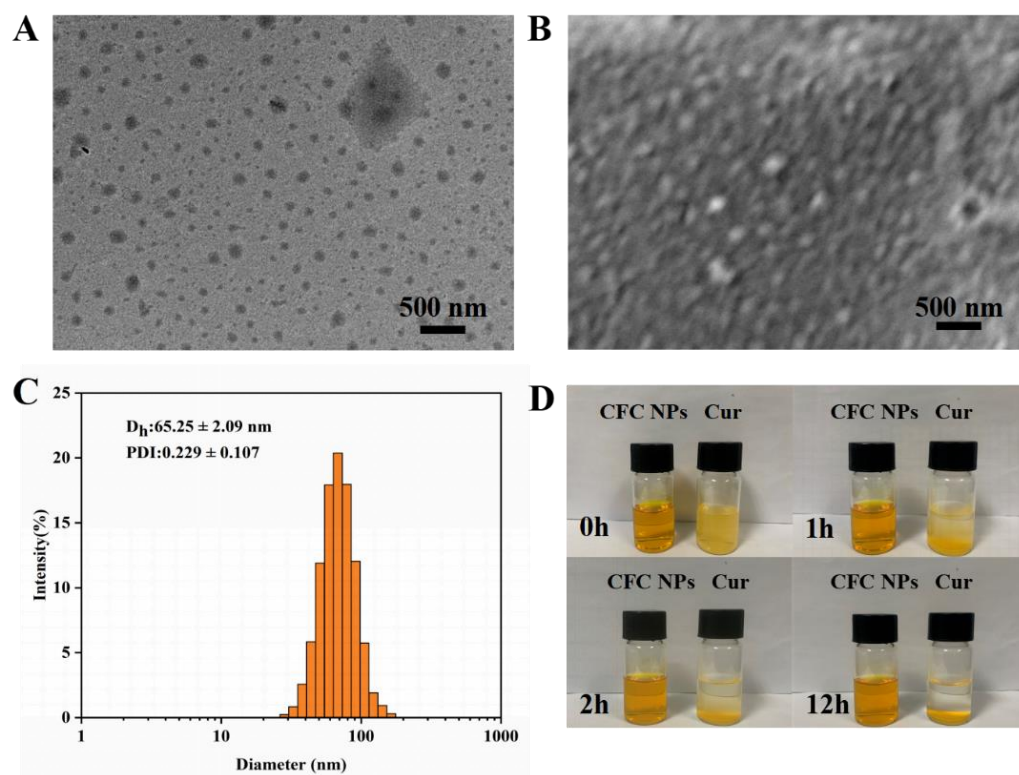


**Figure 1.** (A) TEM image and (B) SEM image of CFC NPs. (C) Particle size distribution and PDI of CFC NPs. (D) Visual appearances of CFC NPs and free Cur during 12 h of storage time.

Storage stability is important for the practical application of CFC NPs in the food industry. The visual appearance of CFC NPs during 12 h of storage time at room temperature was presented in Figure 1D. The aggregates of Cur were formed within 1 h because of their low water solubility of 11 ng/mL [17]. In contrast, the CFC NPs were preserved in a transparent state without obvious precipitation over time, which indicated that CFC NPs were stable under storage conditions. These results might be attributed to the fact that the hydrophilic surface increased the water dispersibility of Cur, and the negative charge of CFC NPs provided the electrostatic repulsion to inhibit the aggregation [18].

## 2.2. UV-Vis and Fluorescence Spectroscopy Analysis

To further investigate the spectral changes of the CFC NPs, the UV-Vis and fluorescence spectra of free Cur and CFC NPs were analyzed. As shown in Figure 2A, the UV-Vis spectra of free Cur and CFC NPs were somewhat different from that of free Cur [19]. The spectrum of CFC NPs showed a slight blue shift, and the maximum absorption spectra of Cur shifted from 423 to 420 nm. A similar behavior was observed in the fluorescence spectra (Figure 2B), where the emission maxima shifted from 595 to 585 nm. The blue shift of the Cur peak could be the result of noncovalent interactions in CFC NPs, such as  $\pi$ - $\pi$  stacking interactions [20]. Notably, the fluorescence intensity of CFC NPs was dramatically decreased compared to that of free Cur, which declared that the collision and aggregation among the CFC NPs seemed to result in fluorescence quenching. These results preliminarily confirmed that CFC NPs were successfully fabricated [21].

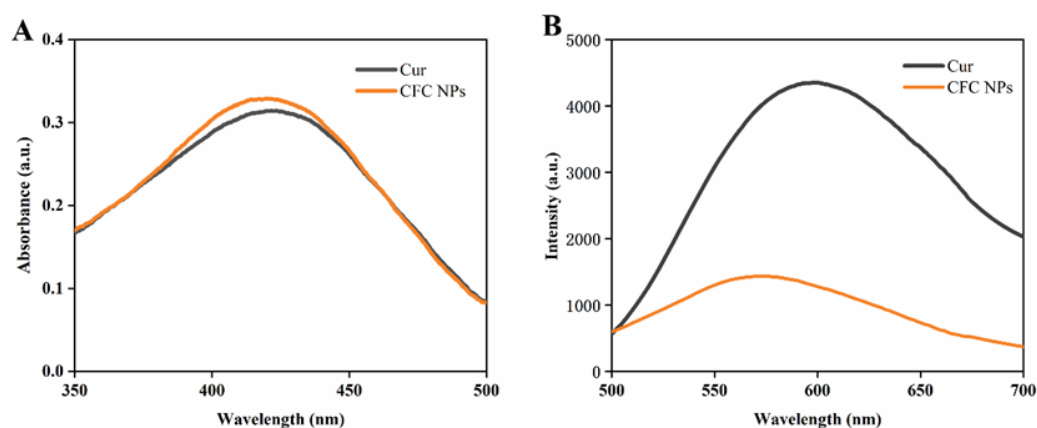


**Figure 2.** (A) UV-Vis absorption spectra and (B) fluorescence spectra of free Cur and CFC NPs.

### 2.3. XRD Analysis

As shown in Figure 3, XRD was carried out on Cur, mPEG-DSPE, a physical mixture of mPEG-DSPE and Cur, and CFC NPs to ascertain the physical state of Cur within CFC NPs. Free Cur was in a highly crystallized state and exhibited many sharp peaks at  $8.78^\circ$ ,  $12.20^\circ$ ,  $14.42^\circ$ ,  $17.14^\circ$ ,  $23.18^\circ$ ,  $24.64^\circ$ ,  $25.62^\circ$ , and  $29.04^\circ$ , which was consistent with previous reports [22]. It should be noted that CFC NPs did not show these sharp characteristic peaks of Cur, which indicates that Cur changed from a crystalline state into an amorphous state after being encapsulated in CFC NPs. In contrast, these diffraction peaks of Cur still existed in the physical mixture. This indicates that the formation of CFC NPs indeed changed the crystalline state of Cur. These results indicated that once encapsulated in CFC NPs, Cur existed in an amorphous state.

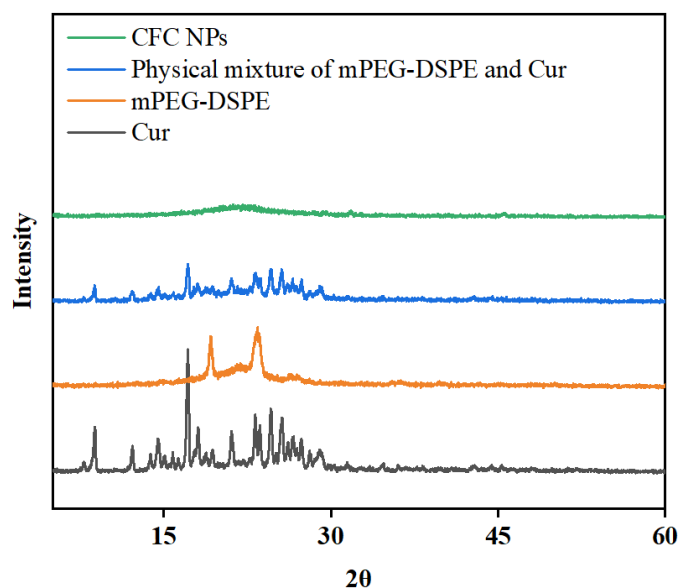


**Figure 3.** X-ray diffraction patterns of CFC NPs, physical mixture of mPEG-DSPE and Cur, mPEG-DSPE, and Cur, respectively.

### 2.4. Photostability Assay

Interlinked 2-hydroxymethoxy benzene rings exist in Cur molecules, which are unstable when exposed to light. Indeed, photochemical degradation is one of the reasons for their loss of biological activity. As demonstrated in Figure 4, the free Cur showed a rapid degradation rate. About 60% of Cur molecules were degraded after 15 min, and only 21% survived after 30 min. In comparison, the CFC NPs showed a retardation phenomenon, and

only 5% of Cur molecules were degraded after 30 min light treatment. The observations clearly indicated that the CFC NPs significantly reduced the degradation rate of Cur and provided better protection under UV light exposure. This would be conducive to the utilization of Cur in the field of functional foods.

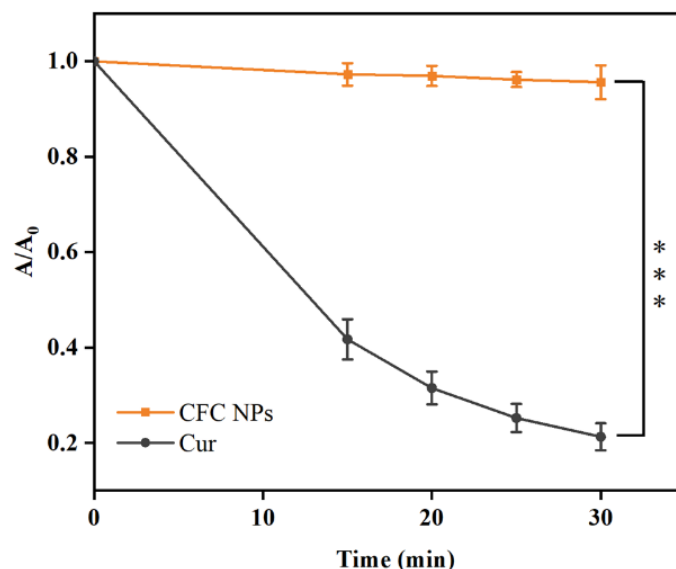


**Figure 4.** Photo-decomposition profiles of CFC NPs and free Cur after UV-light irradiation for 30 min. \*\*\*  $p < 0.001$ .

### 2.5. In Vitro Release Study

The drug release profiles of CFC NPs were shown in Figure 5. Free Cur and CFC NPs exhibited a similar release trend in the SGF and SIF, which referred to a rapid release in SGF and then a relatively slower release in the SIF condition. A burst release occurred in CFC NPs at the beginning of SGF, which was probably related to the dissolution of Cur on the surface of NPs. After 2 h of incubation in SGF, the drug release of CFC NPs was ~31.31%. In contrast, free Cur released at a slow rate (~21.58%) owing to its poor solubility in the gastrointestinal fluid. When the samples were transferred from SGF to SIF, a sustained release of Cur could be clearly observed. After 4 h of incubation in SIF, the cumulative release rate of free Cur and CFC NPs was ~37.35% and ~48.84%, respectively. The CFC NPs showed higher drug release in the SGF and SIF, compared to that of free Cur. This phenomenon is attributed to the larger surface area and the enhanced dispersibility in water. This similar phenomenon was also reported by Xiao et al. [23]. The above results indicated that the formation of CFC NPs successfully promoted the release of Cur in simulated digestive juices, which would allow more Cur to be absorbed by the body.

### 2.6. Antioxidant Activity

Cur, a phenolic compound, has been evidenced to exhibit antioxidant activity through forming phenoxy groups to remove free radicals [24]. The DPPH radical-scavenging method was broadly employed to evaluate antioxidant capacity owing to its cost-effectiveness, high sensitivity, and good reproducibility [25]. As shown in Figure 6, both the CFC NPs and free Cur displayed dose-dependent DPPH radical scavenging activity. At the concentration of 20  $\mu\text{g/mL}$ , the DPPH radical scavenging activities of free Cur and CFC NPs were ~27.95% and ~66.18%, respectively. These results indicated that CFC NPs exhibited a remarkably higher antioxidant activity than that of free Cur. This was attributed to the Cur being encapsulated in CFC NPs with a hydrophilic surface, which provided better contact between Cur and free radicals. Several other studies also reported this similar phenomenon [26–28]. These findings imply that the CFC NPs could be used as antioxidant ingredients in food formulations, which would be beneficial for the human body.

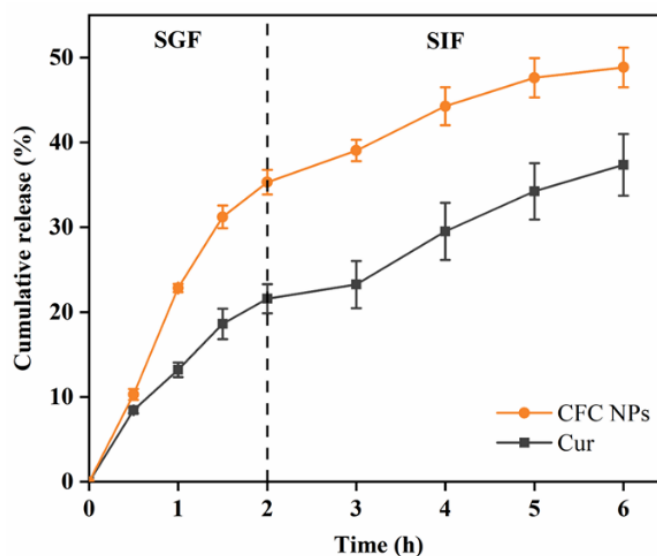


**Figure 5.** In vitro drug release profiles of CFC NPs and free Cur. SGF and SIF represent simulated gastric fluid and simulated intestinal fluid, respectively.

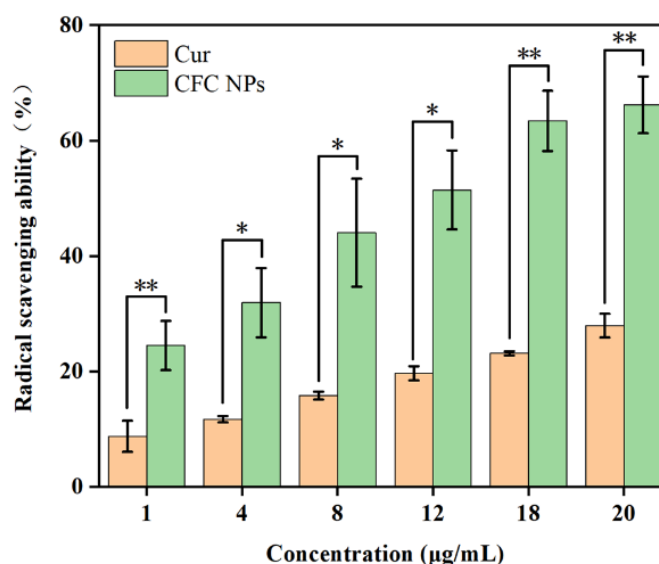


**Figure 6.** DPPH radical scavenging activity of CFC NPs and free Cur. \*  $p < 0.05$ , \*\*  $p < 0.01$ .

### 3. Materials and Methods

#### 3.1. Materials

Curcumin (purity > 97%) was acquired from Dalian Meilun Biotechnology Co., Ltd. (Dalian, China). 1,2-Distearoyl-sn-glycero-3-phosphoethanolamine-*N*-methoxy-poly (ethylene glycol 2000) (mPEG-DSPE) was purchased from Shanghai ToYongBio Tech. Inc., Ltd. (Shanghai, China). All other solvents including dimethyl sulfoxide (DMSO) and ethanol were provided by Sinopharm Chemical Reagent Co., Ltd. (Shanghai, China).

#### 3.2. Preparation of CFC NPs

Briefly, 2 mg of Cur was dissolved in 1 mL of DMSO. Then, 250 µL of the above solution was injected dropwise into 10 mL of DI water under stirring (40 °C). Subsequently, 50 µg of mPEG-DSPE was added. Then, the CFC NPs were finally formed. The DMSO was removed by the dialysis method for the evaluation of subsequent experiments.



### 3.3. Characterization of CFC NPs

The particle size distribution of the newly prepared CFC NPs was measured using dynamic light scattering (Zetasizer Nano-ZS90, Malvern Instruments, Worcestershire, UK). Experimentally, each sample was diluted with deionized water for analysis, and then some of the diluted solution was filtered by a 0.45 µm PES (polyether sulfone) membrane. After filtering, the hydrodynamic diameter and PDI of CFC NPs were measured at 25 °C, and each value was measured at least three times.

Morphology of the formed CFC NPs was investigated with a TEM. A copper grid (400 mesh) was used to carry 200 µL of the sample. The CFC NPs were observed by TEM after drying for 12 h at 25 °C. In addition, the surface morphology of the obtained CFC NPs was observed using an SEM (Hitachi, Tokyo, Japan). CFC NPs were dried on silicon pellet at room temperature. The samples were sputter coated with gold before imaging.

The samples of Cur and freshly prepared CFC NPs were placed in a glass bottle at room temperature. The appearance of samples was recorded at predetermined time intervals (0, 1, 2, and 12 h).

### 3.4. Loading Capacity (LC)

Loading capacity was calculated after determining the concentration of Cur by UV-Vis spectroscopic method. The CFC NPs were firstly centrifuged at  $1000 \times g$  for 10 min. Then, the precipitation resulting from the centrifugation was removed. Liquid supernatant was dissolved using DMSO-water solution (DMSO:H<sub>2</sub>O = 4:1). The above sample was quantified using UV-Vis spectrophotometer at 425 nm. In addition, a Cur calibration curve at different concentrations was obtained:  $Y = 0.1504X + 0.0164$  ( $R^2 = 0.9994$ ), where Y and X refer to the absorbance and concentration of Cur, respectively. The loading capacity (LC) was calculated by the following equation:

$$LC (\%) = (\text{total Cur} - \text{free Cur}) / \text{total amount of nanoparticles} \times 100$$

### 3.5. Spectroscopic Techniques

The UV-Vis absorption spectra of samples were measured in the wavelength range of 350 to 500 nm. The corresponding solution was used for blank correction.

The fluorescence of free Cur and CFC NPs was analyzed via a fluorescence spectrophotometer (Synergy H1, BioTek Instruments, Inc., Winooski, VT, USA). The excitation wavelength of all samples was recorded at 442 nm.

### 3.6. XRD Patterns

The XRD patterns of free Cur, physical mixture of mPEG-DSPE and Cur, mPEG-DSPE, and lyophilized CFC NPs powders were recorded on X-ray diffractometer (Rigaku D/MAX 2500V). The CFC NPs were pre-frozen at −60 °C for 4 h and freeze-dried to obtain the powders of CFC NPs. The obtained samples were determined from 5° to 60° at a speed of 10°/min.

### 3.7. Photostability Assay

Freshly prepared samples of free Cur and CFC NPs were exposed to UV light (254 nm). Then, the samples were irradiated for a certain time (0, 15, 20, 25, and 30 min). The retention rate of Cur was calculated:

$$\text{Retention rate of Cur} = A / A_0$$

where A and A<sub>0</sub> represent the absorbance at different time points and the initial absorbance of Cur, respectively.

### 3.8. In Vitro Simulated Gastrointestinal Studies

The in vitro release of the free Cur and CFC NPs was analyzed using the dialysis bag method. Briefly, the release medium for Cur was obtained by adding SGF or SIF into ethanol. Then, 6 mL of CFC NPs or free Cur solution was added into the dialysis bags (MWCO of 8000–14,000 Da). They were submerged in 100 mL of SGF release medium for 2 h at 37 °C. After that, the dialysis bags were transferred to 100 mL SIF release medium and kept for 4 h at 37 °C. At specific times, 4 mL of sample was collected and replaced with 4 mL of fresh release medium into flask. The percentage of the released drug was obtained by determining the Cur content of the above-collected samples.

### 3.9. Antioxidant Activity

The antioxidant activity of the free Cur and CFC NPs was examined by the method previously described [29]. Initially, DPPH ethanol solution and multiple concentrations of free Cur and CFC NPs were prepared. Then, 1 mL of DPPH ethanol solution was mixed with of sample solution and stored at 25 °C for 30 min in dark condition. Finally, a microplate reader analyzed the absorbance of samples (at 517 nm). Blank solution was also prepared by mixing DPPH ethanol solution with water, and DPPH radical scavenging activity was estimated using the previously reported formula [30,31].

### 3.10. Statistical Analysis

All measurements were repeated at least three times. Data were recorded as mean  $\pm$  standard deviation and statistically analyzed for a significant difference by Graph-Pad Prism 9.3.0.

## 4. Conclusions

In the present work, CFC NPs with a high drug loading capacity ( $96.68 \pm 0.03\%$ ) were successfully fabricated. Various noncovalent interactions might be the dominant driving forces for facilitating the formation of CFC NPs. With the functionalization of biocompatible mPEG-DSPE, the CFC NPs showed excellent water dispersibility and improved antioxidant activity. Meanwhile, the CFC NPs exhibited a small particle size of  $65.25 \pm 2.09$  nm, a zeta potential of  $-20.5 \pm 1.3$  mV, and a spherical shape. Overall, this study provides an effective approach to deliver nutraceuticals, such as Cur, which could be applied in the functional food and pharmaceutical industries.

**Author Contributions:** Conceptualization, F.Y.; methodology, J.W. and J.C.; software, Z.W.; validation, B.L., Q.Q., H.C. and J.L.; formal analysis, Z.W.; investigation, J.W. and J.C.; resources, P.Z. and W.L.; data curation, J.W. and J.C.; writing—original draft preparation, Z.W.; writing—review and editing, F.Y., X.H. and X.D.C.; visualization, F.Y.; supervision, F.Y.; project administration, F.Y.; funding acquisition, F.Y., X.H. and X.D.C. All authors contributed to the article and approved the submitted version. All authors have read and agreed to the published version of the manuscript.

**Funding:** This research was funded by the Natural Science Foundation of Guangxi Province (2020-GXNSFBA297131 and AD21220026) and the Particle Engineering Laboratory at Soochow University.

**Institutional Review Board Statement:** Not applicable.

**Informed Consent Statement:** Not applicable.

**Data Availability Statement:** The data presented in this study are available from the corresponding author upon request.

**Conflicts of Interest:** The authors declare no conflict of interest.

**Sample Availability:** Not available.



## References

1. Ubeyitogullari, A.; Ciftci, O.N. A novel and green nanoparticle formation approach to forming low-crystallinity curcumin nanoparticles to improve curcumin's bioaccessibility. *Sci. Rep.* **2019**, *9*, 19112. [\[CrossRef\]](#)
2. Mahmood, K.; Zia, K.M.; Zuber, M.; Salman, M.; Anjum, M.N. Recent developments in curcumin and curcumin based polymeric materials for biomedical applications: A review. *Int. J. Biol. Macromol.* **2015**, *81*, 877–890. [\[CrossRef\]](#) [\[PubMed\]](#)
3. Rafiee, Z.; Nejatian, M.; Daeihamed, M.; Jafari, S.M. Application of different nanocarriers for encapsulation of curcumin. *Crit. Rev. Food Sci. Nutr.* **2019**, *59*, 3468–3497. [\[CrossRef\]](#) [\[PubMed\]](#)
4. Karaosmanoglu, S.; Zhou, M.; Shi, B.; Zhang, X.; Williams, G.R.; Chen, X. Carrier-free nanodrugs for safe and effective cancer treatment. *J. Control Release* **2021**, *329*, 805–832. [\[CrossRef\]](#) [\[PubMed\]](#)
5. Guo, Y.; Jiang, K.; Shen, Z.; Zheng, G.; Fan, L.; Zhao, R.; Shao, J. A Small Molecule Nanodrug by Self-Assembly of Dual Anticancer Drugs and Photosensitizer for Synergistic Near-Infrared Cancer Theranostics. *ACS Appl. Mater. Interfaces* **2017**, *9*, 43508–43519. [\[CrossRef\]](#) [\[PubMed\]](#)
6. Zhang, H.; Zhang, Y.; Chen, Y.; Zhang, Y.; Wang, Y.; Zhang, Y.; Song, L.; Jiang, B.; Su, G.; Li, Y.; et al. Glutathione-responsive self-delivery nanoparticles assembled by curcumin dimer for enhanced intracellular drug delivery. *Int. J. Pharm.* **2018**, *549*, 230–238. [\[CrossRef\]](#)
7. Etter, E.L.; Mei, K.C.; Nguyen, J. Delivering more for less: Nanosized, minimal-carrier and pharmacoeactive drug delivery systems. *Adv. Drug Deliv. Rev.* **2021**, *179*, 113994. [\[CrossRef\]](#)
8. Yuan, Y.; Xiao, J.; Zhang, P.; Ma, M.; Wang, D.; Xu, Y. Development of pH-driven zein/tea saponin composite nanoparticles for encapsulation and oral delivery of curcumin. *Food Chem.* **2021**, *364*, 130401. [\[CrossRef\]](#)
9. Chang, C.; Meikle, T.G.; Su, Y.; Wang, X.; Dekiwadia, C.; Drummond, C.J.; Conn, C.E.; Yang, Y. Encapsulation in egg white protein nanoparticles protects anti-oxidant activity of curcumin. *Food Chem.* **2019**, *280*, 65–72. [\[CrossRef\]](#)
10. Zhao, Y.; Zhao, Y.; Ma, Q.; Zhang, H.; Liu, Y.; Hong, J.; Ding, Z.; Liu, M.; Han, J. Novel carrier-free nanoparticles composed of 7-ethyl-10-hydroxycamptothecin and chlorin e6: Self-assembly mechanism investigation and in vitro/in vivo evaluation. *Colloids Surf. B Biointerfaces* **2020**, *188*, 110722. [\[CrossRef\]](#)
11. Zhi, K.; Wang, R.; Wei, J.; Shan, Z.; Shi, C.; Xia, X. Self-assembled micelles of dual-modified starch via hydroxypropylation and subsequent debranching with improved solubility and stability of curcumin. *Food Hydrocoll.* **2021**, *118*, 106809. [\[CrossRef\]](#)
12. Fan, L.; Zhang, B.; Xu, A.; Shen, Z.; Guo, Y.; Zhao, R.; Yao, H.; Shao, J.W. Carrier-Free, Pure Nanodrug Formed by the Self-Assembly of an Anticancer Drug for Cancer Immune Therapy. *Mol. Pharm.* **2018**, *15*, 2466–2478. [\[CrossRef\]](#)
13. Deka, S.R.; Yadav, S.; Kumar, D.; Garg, S.; Mahato, M.; Sharma, A.K. Self-assembled dehydropeptide nano carriers for delivery of ornidazole and curcumin. *Colloids Surf. B Biointerfaces* **2017**, *155*, 332–340. [\[CrossRef\]](#)
14. Feng, B.; Niu, Z.; Hou, B.; Zhou, L.; Li, Y.; Yu, H. Enhancing Triple Negative Breast Cancer Immunotherapy by ICG-Templated Self-Assembly of Paclitaxel Nanoparticles. *Adv. Funct. Mater.* **2020**, *30*, 1906605. [\[CrossRef\]](#)
15. Shehzad, Q.; Rehman, A.; Jafari, S.M.; Zuo, M.; Khan, M.A.; Ali, A.; Khan, S.; Karim, A.; Usman, M.; Hussain, A.; et al. Improving the oxidative stability of fish oil nanoemulsions by co-encapsulation with curcumin and resveratrol. *Colloids Surf. B Biointerfaces* **2021**, *199*, 111481. [\[CrossRef\]](#) [\[PubMed\]](#)
16. Urmi, W.T.; Rahman, M.M.; Kadrigama, K.; Ramasamy, D.; Maleque, M.A. An overview on synthesis, stability, opportunities and challenges of nanofluids. *Mater. Today Proc.* **2021**, *41*, 30–37. [\[CrossRef\]](#)
17. Kaminaga, Y.; Nagatsu, A.; Akiyama, T.; Sugimoto, N.; Yamazaki, T.; Maitani, T.; Mizukami, H.J.F. Production of unnatural glucosides of curcumin with drastically enhanced water solubility by cell suspension cultures of *Catharanthus roseus*. *FEBS Lett.* **2003**, *555*, 311–316. [\[CrossRef\]](#)
18. Saputra, O.A.; Wibowo, F.R.; Lestari, W.W. High storage capacity of curcumin loaded onto hollow mesoporous silica nanoparticles prepared via improved hard-templating method optimized by Taguchi DoE. *Eng. Sci. Technol. Int. J.* **2022**, *33*, 101070. [\[CrossRef\]](#)
19. Kumar Tyagi, P.; Sharma, S.; Tyagi, S.; Mishra, A.; Gola, D. Toxicity assessment of silica nanoparticles, and their conjugates with curcumin on *Drosophila melanogaster*. *Environ. Nanotechnol. Monit. Manag.* **2022**, *17*, 100616. [\[CrossRef\]](#)
20. Acevedo-Guevara, L.; Nieto-Suaza, L.; Sanchez, L.T.; Pinzon, M.I.; Villa, C. Development of native and modified banana starch nanoparticles as vehicles for curcumin. *Int. J. Biol. Macromol.* **2018**, *111*, 498–504. [\[CrossRef\]](#)
21. Periyathambi, P.; Hemalatha, T. Development of water-soluble curcumin grafted magnetic nanoparticles for enhancing bioavailability, fluorescence, and magnetic resonance imaging activity. *Mater. Lett.* **2021**, *294*, 129763. [\[CrossRef\]](#)
22. Dai, L.; Wei, Y.; Sun, C.; Mao, L.; McClements, D.J.; Gao, Y. Development of protein-polysaccharide-surfactant ternary complex particles as delivery vehicles for curcumin. *Food Hydrocoll.* **2018**, *85*, 75–85. [\[CrossRef\]](#)
23. Xiao, J.; Nian, S.; Huang, Q. Assembly of kafirin/carboxymethyl chitosan nanoparticles to enhance the cellular uptake of curcumin. *Food Hydrocoll.* **2015**, *51*, 166–175. [\[CrossRef\]](#)
24. Slavova-Kazakova, A.; Janiak, M.A.; Sulewska, K.; Kancheva, V.D.; Karamac, M. Synergistic, additive, and antagonistic antioxidant effects in the mixtures of curcumin with (–)-epicatechin and with a green tea fraction containing (–)-epicatechin. *Food Chem.* **2021**, *360*, 129994. [\[CrossRef\]](#)
25. Xiang, H.; Sun-waterhouse, D.; Cui, C.; Wang, W.; Dong, K. Modification of soy protein isolate by glutaminase for nanocomplexation with curcumin. *Food Chem.* **2018**, *268*, 504–512. [\[CrossRef\]](#)

26. Chen, S.; Li, Q.; McClements, D.J.; Han, Y.; Dai, L.; Mao, L.; Gao, Y. Co-delivery of curcumin and piperine in zein-carrageenan core-shell nanoparticles: Formation, structure, stability and in vitro gastrointestinal digestion. *Food Hydrocoll.* **2020**, *99*, 105334. [\[CrossRef\]](#)
27. Ak, T.; Gulcin, I. Antioxidant and radical scavenging properties of curcumin. *Chem. Biol. Interact.* **2008**, *174*, 27–37. [\[CrossRef\]](#)
28. Rao, C.; Li, M.; Sun, X.; Li, M.; Lian, X.; Wang, H.; Lan, J.; Niu, B.; Li, W. Preparation and characterization of phosphate-stabilized amorphous calcium carbonate nanoparticles and their application in curcumin delivery. *Mater. Chem. Phys.* **2020**, *255*, 123552. [\[CrossRef\]](#)
29. Shen, W.; Yan, M.; Wu, S.; Ge, X.; Liu, S.; Du, Y.; Zheng, Y.; Wu, L.; Zhang, Y.; Mao, Y. Chitosan nanoparticles embedded with curcumin and its application in pork antioxidant edible coating. *Int. J. Biol. Macromol.* **2022**, *204*, 410–418. [\[CrossRef\]](#)
30. Meng, R.; Wu, Z.; Xie, Q.T.; Cheng, J.S.; Zhang, B. Preparation and characterization of zein/carboxymethyl dextrin nanoparticles to encapsulate curcumin: Physicochemical stability, antioxidant activity and controlled release properties. *Food Chem.* **2021**, *340*, 127893. [\[CrossRef\]](#)
31. Niu, F.; Hu, D.; Gu, F.; Du, Y.; Zhang, B.; Ma, S.; Pan, W. Preparation of ultra-long stable ovalbumin/sodium carboxymethylcellulose nanoparticle and loading properties of curcumin. *Carbohydr. Polym.* **2021**, *271*, 118451. [\[CrossRef\]](#) [\[PubMed\]](#)

**Disclaimer/Publisher’s Note:** The statements, opinions and data contained in all publications are solely those of the individual author(s) and contributor(s) and not of MDPI and/or the editor(s). MDPI and/or the editor(s) disclaim responsibility for any injury to people or property resulting from any ideas, methods, instructions or products referred to in the content.